M. Baranska[1,2]
H. Schulz[1]
S. Reitzenstein[3]
U. Uhlemann[3]
M. A. Strehle[3]
H. Krüger[1]
R. Quilitzsch[1]
W. Foley[4]
J. Popp[3]

[1] *Federal Centre for Breeding Research on Cultivated Plants (BAZ), Institute for Plant Analysis, Neuer Weg 22-23, D-06484 Quedlinburg, Germany*

[2] *Faculty of Chemistry, Jagiellonian University, Ingardena 3, 30-060 Krakow, Poland*

[3] *Institut für Physikalische Chemie, Friedrich-Schiller-Universität Jena, Helmholtzweg 4, D-07743 Jena, Germany*

[4] *School of Botany and Zoology, Australian National University, Canberra 0200, Australia*

Vibrational Spectroscopic Studies to Acquire a Quality Control Method of Eucalyptus Essential Oils

Abstract: *This article presents a novel and original approach to analyze in situ the main components of* Eucalyptus *oil by means of Raman spectroscopy. The obtained two-dimensional Raman maps demonstrate a unique possibility to study the essential oil distribution in the intact plant tissue. Additionally, Fourier Transform (FT)-Raman and attenuated total reflection (ATR)-IR spectra of essential oils isolated from several* Eucalyptus *species by hydrodistillation are presented. Density Functional Theory (DFT) calculations were performed in order to interpret the spectra of the essential oils of the* Eucalyptus *species. It is shown that the main components of the essential oils can be recognized by both vibrational spectroscopic techniques using the spectral information of the pure terpenoids. Spectroscopic analysis is based on the key bands of the individual volatile substances and therefore allows one to discriminate different essential oil profiles of several* Eucalyptus *species. It has been found that the presented spectroscopic data correlate very well with those obtained by gas chromatography (GC) analysis. All these investigations are helpful tools to generate a fast and easy method to control the quality of the essential oils with vibrational spectroscopic techniques in combination with DFT calculations.* © 2005 Wiley Periodicals, Inc. Biopolymers 78: 237–248, 2005

This article was originally published online as an accepted preprint. The "Published Online" date corresponds to the preprint version. You can request a copy of the preprint by emailing the Biopolymers editorial office at biopolymers@wiley.com

Keywords: *essential oil;* Eucalyptus; *attenuated total reflection–infrared; Raman mapping in situ*

INTRODUCTION

Eucalyptus species are fast growing trees exploited mainly for paper pulp but also as a source for various essential oils. For the production of phytopharmaceuticals, essential oils rich in 1,8-cineole (called also "eucalyptol"), are of special importance.[1] These products are applied for relief of head colds, rheumatism, muscular pain, and as expectorant in cases of bronchitis (added to cough syrups). There exist 20 or more species of *Eucalyptus* used for the production of this type of oil, among them are *E. polybractea* and *E. globulus*. In turn, eucalyptus oil isolated from the leaves of *E. gunnii* has been reported to have antifungal properties.[1] The essential oil of *E. citriodora* appears to have bacteriostatic activity toward *Staphylococcus aureus* due to synergism between citronellol and citronellal present in the oil. The volatile components of *E. globulus* show antiseptic properties and can be used for treatment of gum disease known as "pyorrhoea" and may be applied on burns to prevent infections.[1] Jensenone, the main component of *E. jensenii*, shows antifeedant actions due to the presence of aldehyde and phenol groups.[2,3]

Up to now, gas chromatographic (GC) methods have been extensively applied for the determination of individual components of essential oils. Identification of terpenoids can be performed using standard detectors such as GC-FID (flame ionization detection) as well as more sophisticated techniques like GC-MS (mass spectroscopy)[4–6] and GC-FTIR-MS (FTIR: Fourier transform infrared).[7] Also, Solid Phase Microextraction (SPME)-GC as an efficient clean-up technique[9] has been reported for the analysis of *Eucalyptus* oil. Alternatively, different vibrational spectroscopic methods were successfully applied for the identification of the main compounds in the isolated essential oil and for the discrimination of different species of various spice plants.[10–16]

However, the isolation of essential oil by hydrodistillation or solvent extraction may lead to changes with regard to composition and quality. Therefore, the in situ analysis of essential oils that does not cause artefacts of the analytes is of great interest.[11] In combination with Raman, mapping techniques are a powerful tool to study the chemical composition of plant samples not only in a single point but also within a larger area.[17–20]

The purpose of this study was to determine the chemical composition of various *Eucalyptus* oils isolated from several species by using standard GC methods as well as ATR-IR and NIR-FT-Raman (NIR: near infrared) spectroscopy. Additionally, micro Raman spectroscopy was used for in situ investigation of the main components of *Eucalyptus* oil droplets as well as to provide detailed information about their spatial distribution. The goal of this study is the establishment of a sophisticated quality control method based on vibrational spectroscopy.

EXPERIMENTAL

Samples and Reference Analysis

Most of the analyzed eucalyptus leaves were collected in Australia. Additionally, two species, *E. cinerea* and *E. globulus*, were obtained from the Botanical Garden in Jena (Germany).

The isolation of essential oils from *Eucalyptus* leaves was performed using the classical method of hydrodistillation described in the European Pharmacopoeia.[21] The obtained oils were analyzed by gas chromatography/flame ionization detection (GC/FID) using a Hewlett-Packard gas chromatograph 5890 series II, fitted with an HP-Innowax column (60 m × 0.25 mm i.d.; film thickness 0.5 μm). Detector and injector temperature were set at 280 and 250°C, respectively. The following oven temperature regime was used: from 80 to 120°C at 4°/min and then at 10°/min up to 220°C, the final temperature was held for 40 min (total oven program = 60 min). Carrier gas was hydrogen with a constant flow rate of 1 mL/min (split 1:40). GC-MS analyses of the isolated essential oils were performed using a Hewlett Packard MSD 5972/HP 5890 series plus 2, equipped with a 30 m × 0.25 mm i.d., 0.5 μm HP-Innowax column. Detector and injector temperature were set at 280 and 250°C, respectively. The following oven temperature regime was used: from 80 to 120°C at 4°/min and then at 10°/min up to 220°C, the final temperature was held for 30 min (total oven program = 50 min). Carrier gas was helium with a constant flow rate of 1 mL/min (split 1:20). The ionization energy was set at 70 eV.

Identification of the most detected compounds was based on their relative retention time in comparison to pure standard substances. The other analytes were tentatively identified by using the NBS75K and Wiley 138 library databases of the GC-MS system. The percentage composition was computed from the GC peak areas according to the 100% method without using any correction factors.

Vibrational Spectroscopic Measurements

Near Infrared-Fourier Transform-Raman (NIR-FT-Raman) Spectroscopy. NIR-FT-Raman spectra were recorded using a Bruker Spectrometer (model RFS 100) equipped with a Neodynium : Yttrium Aluminum Garnet (Nd : YAG) laser, emitting at 1064 nm, and a germanium detector cooled with liquid nitrogen. The instrument was equipped with a *xy* stage, a mirror objective, and a prism slide for redirection of the laser beam. In contrast to the standard vertical sampling arrangement, the samples were mounted horizontally.

Spectral data of the individual isolated *Eucalyptus* oils (sample amount: approximately 3–5 μL) were accumulated

from 128 scans with a spectral resolution of 4 cm^{-1} in the range of 1000–4000 cm^{-1} with a laser power of 100 mW supplied by a unfocused laser beam.

Two-dimensional (2D) Raman maps of *Eucalyptus* leaves were obtained point by point by moving the *xy* stage; *x* and *y* directions of the accessory were controlled by the spectrometer software. Traces or 2D surface areas of the mapped samples were processed by the Bruker Opus/map software package. Raman mapping of an *Eucalyptus globulus* leaf was performed at an area of 1.2 × 1.3 mm with a spatial resolution of 40 μm. The sample was irradiated with a focused laser beam of 50 mW showing a diameter of about 0.1 mm. The spectral resolution was 4 cm^{-1}; 12 scans were collected at each measured point.

Dispersive Raman Spectroscopy. The Raman spectra were recorded with a micro Raman setup (LabRam inverse, Jobin–Yvon–Horiba). The focal length of the spectrometer is 800 mm and is equipped with a 300-lines/mm grating. The 830.15 nm line of a diode laser with a laser power of 8 mW incident on the sample was used as excitation wavelength. The scattered light was detected by a CCD camera operating at 220 K.

A mobile micro Raman setup was developed in order to perform field experiments. The apparatus consisted of two modules, a microscope module and a spectrometer module as well as the necessary electronics and a computer. The spectrometer module consisted of a laser and a spectrometer. As excitation wavelength, the 785-nm line of a Toptica Xtra diode laser was used. The spectrometer was equipped with a Wright CCD camera operating at 220 K. The laser beam was guided by an optical fiber to the microscope and the Raman scattered light was guided in an optical fiber to the spectrometer. The microscope consisted of a modified Olympus BX41 microscope with an Olympus MIRPlan 20× microscope objective. To avoid exposure to daylight, the microscope module was encased by a black cover with a door that could be opened for the sample placement at the microscopic table and that could be closed for the measurements.

The sample transportation and therefore the manipulation of the sample are reduced to a minimum, which is the main advantage of such an apparatus.

Attenuated Total Reflection Infrared (ATR-IR) Spectroscopy. The mid-infrared spectra were recorded in the range between 650 and 4000 cm^{-1} on an EQUINOX spectrometer (Bruker, Germany) in a 9-reflection configuration using a diamond–ZnSe–ATR crystal. Approximately 5–10 μL of the essential oil were placed on the surface of the ATR crystal. The spectra were accumulated from 30 scans with a spectral resolution of 4 cm^{-1}.

DFT Calculations

DFT calculations of jensenone were performed with the B3LYP functional and the 6-31G(d) using Gaussian03.[22] Vibrational frequencies were scaled with a factor of 0.9614.[23]

RESULTS AND DISCUSSION

Discrimination of *Eucalyptus* Species Based on GC Data (Essential Oil Profiles)

Table I shows the main components of the analysed *Eucalyptus* oils identified and quantified by GC according to the 100% GC method. The molecular structures of the main substances detected in these oils are presented in Figure 1. The GC data allows us to discriminate between the different types of investigated oils based on their predominant components and characteristic profiles. Oils of *E. polybractea*, *E. loxophleba*, *E. nortonii*, *E. globulus*, and *E. cinerea* belong to the 1,8-cineole type containing this component in amounts between 60 and 80%. The citronellal type can be singled out for *Eucalyptus citriodora* with a citronellal content of 78 and 11% of citronellol. For the other *Eucalyptus* oils, the following classification can be performed (amounts of main components are given in parentheses): *E. macarthurii*—geranyl acetate type (36%); *E. elata*—menthen-ol type (43%); *E. torquata*—torquatone type (34%); and *E. crenulata*—phenylethyl phenylacetate type (45%). The composition of *Eucalyptus jensenii* essential oil shows the highest content of torquatone (26.7%) whereas jensenone is present only in amounts of 14%. The tentative identification of these components was performed by interpretation of their MS spectra because both components are neither included in the GC-MS libraries nor available as standards. The molecule (M^{+1}) ion for torquatone and jensenone was detected at *m/z* = 280 and 266, respectively, and after fragmentation the intensive peak appears at 223 and 209, respectively. That corresponds to the separation of a —CH$_2$—CH—(CH$_3$)$_2$ group from the molecule. Despite torquatone being the most abundant component in *E. jensenii* oil, the presence of jensenone leads to a classification as the jensenone type. From the literature it is known that this component can occur in *E. jensenii* oil in a much higher content, even in amounts of 70%.[24]

Vibrational Spectroscopic Features of *Eucalyptus* Oil

Detailed spectral analysis of the investigated oils is based on their vibrational spectra. First of all, the FT-Raman and ATR-IR spectra of available terpenoid compounds, which are present in *Eucalyptus* essential oils in higher amounts, were recorded. Some of them have already been published and discussed.[25,26] Based on these data, assignment of the most intensive bands to be seen in the spectra of the investigated oils

Table I Main Components of the Essential Oils Obtained from Different *Eucalyptus* Species Measured by GC (Only Components > 4% GC Are Listed)

Eucalyptus Species	Composition (%)
E. jensenii	26.7 Torquatone, 14.0 jensenone, 7.1 isotorquatone, 4.9 globulol, 4.4 spathulenol, 4.2 α-pinene, 4.2 α-terpineol, 4.1 verdiflorol
E. macarthurii	36.2 Geranyl acetate, 22.9 β-eudesmol, 18.2 α-eudesmol, 6.5 γ-eudesmol, 4.9 geraniol
E. elata	43,4 δ-2-*p*-Menthen-ol, 17.0 piperitol, 11.7 *p*-cymene, 5.7 β-phellandrene, 4.8 terpinen-4-ol
E. torquata	42.0 Torquatone, 11.2 1,8-cineole, 10.2 α-pinene, 10.2 α-eudesmol, 11.1 β-eudesmol, 4.8 γ-eudesmol
E. citriodora	77.8 Citronellal, 10.8 citronellol, 6.9 neo-isopulegol
E. crenulata	45.1 Phenylethyl phenylacetate, 17.3 γ-terpinene, 14.7 *p*-cymene, 7.8 ocimene
E. polybractea	80.2 1,8-Cineole
E. loxophleba	66.0 1,8-Cineole, 17.3 α-pinene, 6.4 limonene
E. nortonii	60.0 1,8-Cineole, 9.0 α-terpineol, 6.3 limonene, 5.8 globulol
E. globulus	[a]63.0 1,8-cineole, 23.5 α-pinene, 6.2 limonene 51.0 1,8-cineole, 16.7 α-pinene, 6.2 limonene, 7.3 globulol
E. cinerea	[a]57.5 1,8-cineole, 9.3 terpenylacetate, 9.2 α-pinene, 6.2 limonene

[a] Essential oil obtained by microdistillation.

(Figure 2) was performed and collected in Table II.[27] All spectra show characteristic key bands that can be used for discrimination of the species *E. jensenii, E. macarthurii, E. elata, E. torquata, E. citriodora, E. crenulata*, and *E. polybractea* based on their essential oils. These *Eucalyptus* oils show different spectra both in Raman and in ATR-IR.

The FT-Raman spectrum of *E. jensenii* oil is dominated by a strong band at 1625 cm^{-1}, which can be assigned to a stretching vibration of the jensenone aromatic ring. This band can also be seen in the corresponding ATR-IR spectrum but is here overlapped by a signal at 1593 cm^{-1}. DFT calculations indicate that the peak at 1593 cm^{-1} can be assigned to a carbonyl vibration that occurs at an untypically low wavenumber. This interpretation is in accordance to the article by Zborowski et al.[28]

An additional intense mode is observed at 1190 cm^{-1}, which can be assigned to a C—C—O stretching vibration of jensenone. It is surprising that although jensenone is present in *E. jensenii* oil in lower amounts than torquatone, the latter is hardly detectable in the spectra presented in Figure 2. The explanation can be taken from Figure 3, where the Raman spectrum of *E. jensenii* (a) and *E. torquata* (b) oils are presented in the wavenumber range from 300 to 3800 cm^{-1}. Torquatone as a main component of *E. torquata* oil contributes to the intensive signals due to C—H stretching vibrations at 2958, 2920, and 2871 cm^{-1}, and these bands can also be seen in *E. jensenii* oil. However, these bands cannot be used for identification purposes because most terpenes have intense signals in this wavenumber region. On the other hand, the lower wavenumber range of the Raman spectrum obtained from *E. torquata* oil does not show any characteristic bands that could be used for recognition of torquatone. An intensive band detected at about 1450 cm^{-1} is due to deformation vibrations of CH$_3$ and CH$_2$ groups, but again it is not specific for torquatone. The ATR-IR spectrum of *E. torquata* oil in the range between 650 and 1850 cm^{-1} (see Figure 2) reveals bands that can be clearly assigned to torquatone. A broad signal at 1702 cm^{-1} is caused by the stretching vibration of the ketone group whereas at 1109 cm^{-1} an intensive mode due to stretching of C—O—C is seen. Additional components of *E. torquata* oil are detected in the Raman spectrum at 1659 and 666 cm^{-1} (α-pinene) and at 652 cm^{-1} (1,8-cineole). In the ATR-IR spectrum at 984 cm^{-1}, a characteristic signal of 1,8-cineole can be identified (see Table II for details).

The presence of geranyl acetate as a main component of *E. macarthurii* oil is evident from its ATR-IR spectrum where intensive signals can be seen at 1738 and 1365 cm^{-1}. The first one can be attributed to a stretching vibration of the C=O group whereas the second one is due to the CH$_3$ symmetrical deformation mode of the CH$_3$(C=O) group. Additionally, asymmetrical and symmetrical stretching vibrations of C—O—C are recognized at 1227 and 1021 cm^{-1}, respectively. In the Raman spectrum the dominating band at 1672 cm^{-1} is related to the stretching mode of the C=C group.

Both vibrational spectra of *E. elata* oil reflect its complex composition. The main component, 2-*p*-menthen-ol-1, can be identified in the Raman spectrum by the strong signal at 1640 cm^{-1} [ν(C—C)] and in the ATR-IR at 1367 cm^{-1} [δ(C—O—H] and at 1123 cm^{-1} [ν(C—C—O)]. As can be seen in Figure 2, additional intensive bands in the FT-Raman spectrum can be attributed to terpinen-4-ol (1679 and 730 cm^{-1}) and *p*-cymene (1208 and 804 cm^{-1}), whereas in the ATR-IR spectrum terpinene-4-ol is seen at 924 cm^{-1} (see Table II for details).
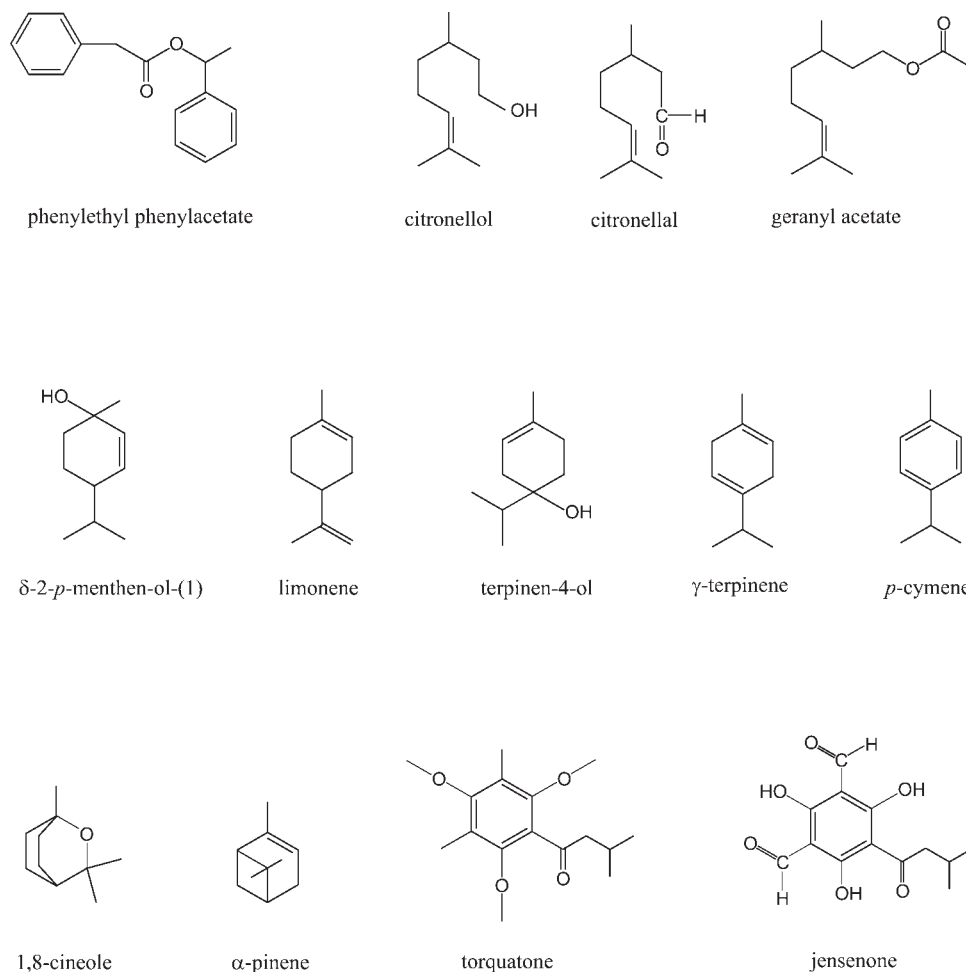
FIGURE 1 Molecular structures of main substances detected in *Eucalyptus* oils.

Spectra of *E. citriodora* oil are dominated by various vibrational modes of citronellal (78%) with some contribution of citronellol (11%). Citronellal can be identified by the stretching mode of C=O at 1725 cm^{-1} (Raman and ATR-IR) and additionally by the stretching vibration of C=C at 1674 cm^{-1} (Raman) as well as a CH$_3$ symmetrical deformation vibration occurring at 1382 cm^{-1} (Raman). Citronellol also contributes to the intensive signals at 1674 and 1382 cm^{-1} (Raman), but in ATR-IR it gives additionally a characteristic band at 1377 cm^{-1} due to deformation of the C—O—H group.

The main component of *E. crenulata* oil, phenylethyl phenylacetate, is well recognizable by its key bands in the Raman spectrum at 1605, 1203, and a very strong signal at 1003 cm^{-1} (ring deformation). In the ATR-IR spectrum, intensive stretching vibration of C=O can be seen at 1736 cm^{-1}; additional bands can be attributed to *p*-cymene (1613, 1208, and 803 cm^{-1}, Raman) and γ-terpinene (1701 and

756 cm^{-1}, Raman and 947 cm^{-1}, ATR-IR) (see Table II for details).

Oils from *E. polybractea, E. loxophleba, E. nortonii, E. globulus*, and *E. cinerea* are related to the 1, 8-cineole type, and accordingly, this component is mainly seen in their vibrational spectra. This bicyclo-camphane compound is clearly observed in the Raman spectrum where it demonstrates a strong ring vibration at 652 cm^{-1}. In the ATR-IR spectrum it can be identified by the most intensive band at 984 cm^{-1} due to a CH$_2$ wagging vibration. Other characteristic but less intensive bands of 1,8-cineole are seen in the ATR-IR spectrum, which can be assigned to C—O—C symmetrical (1079 cm^{-1}) and asymmetrical (1214 cm^{-1}) stretching vibrations as well as to CH$_3$ symmetrical deformation modes recognized at 1374 cm^{-1} (see Table II). Oil components occurring beside 1,8-cineole in lower amount can also be distinguished by their key bands in the Raman spectrum, e.g., α-pinene is seen at 667 and 1659 cm^{-1}in
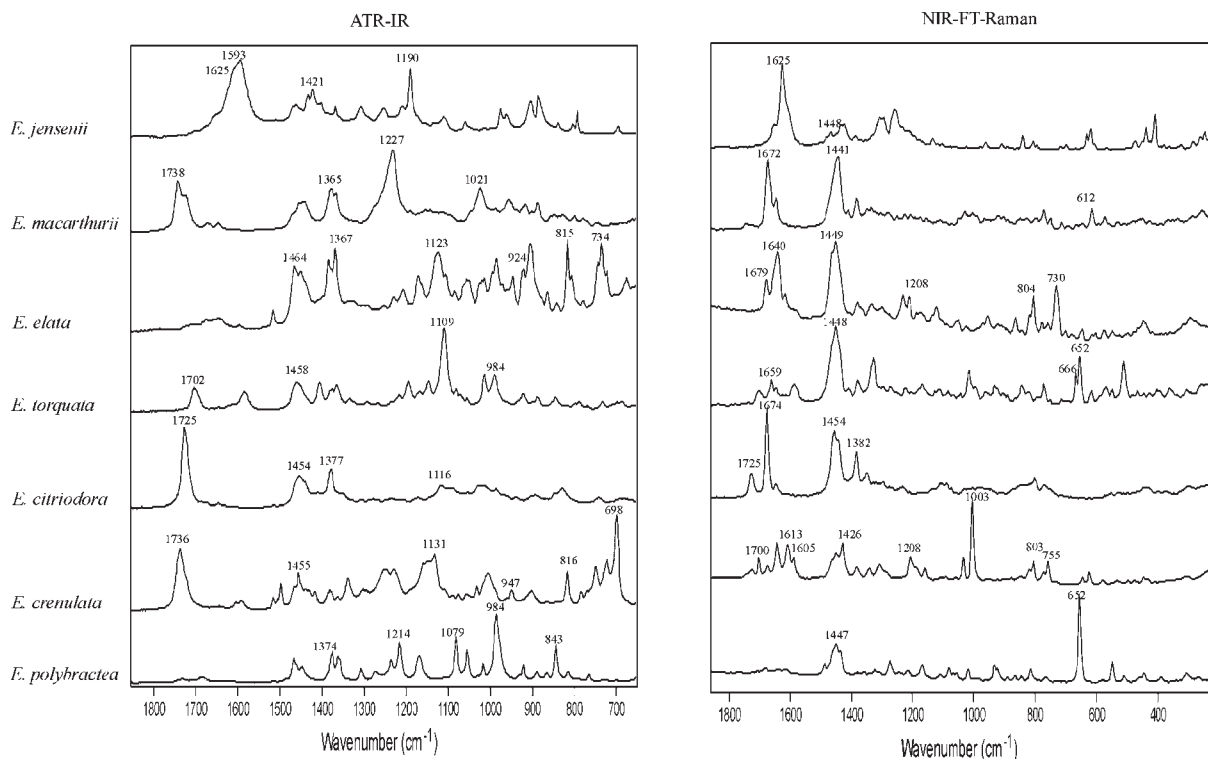
FIGURE 2 ATR-IR and NIR-FT-Raman spectra of essential oils isolated by hydrodistillation from the leaves of different *Eucalyptus* species: *E. jensenii; E. macarthurii, E. elata, E. torquata, E. citriodora, E. crenulata, E. polybractea.*

E. loxophleba and *E. globulus* oil whereas limonene can be detected at 760 and 1678 cm^{-1} in the essential oils of *E. loxophleba, E. nortonii*, and *E. globulus.*

In order to show that it is possible to investigate the composition of essential oils by means of Raman spectroscopy, the Raman spectrum of the essential oil of *Eucalyptus loxophleba* was decomposed into its main components. To this end, the spectra of the pure standard substances 1,8-cineole, α-pinene, and limonene, known as the main components of the essential oil (about 90%, see Table I), are combined in a weighted sum fitted to the measured Raman spectrum of *E. loxophleba*. Raman intensities depend linearly on the sample concentration and on the Raman scattering cross section. Therefore, to make the weighting factors comparable to the contents obtained with GC, the Raman scattering cross sections of the various ingredients had to be approximated. This was done by integrating over the complete spectral range (200–4000 cm^{-1}) of each of the four spectra being recorded under identical experimental conditions and dividing the spectrum by their number. Figure 4 shows the Raman spectra of 1,8-cineole (a), α-pinene (b), and limonene (c). The measured Raman spectrum of *Eucalyptus loxophleba* is shown in Figure 4d. The spectrum, that is

the result of the fit of 1,8-cineole, α-pinene, and limonene to the *E. loxophleba* Raman spectrum, is shown in Figure 4e. The similarity between spectra 4d and 4e is very high. The difference spectrum between the measured and the fitted spectrum is shown in Figure 4f. There are just two weak features in the difference spectrum at 1446 and 652 cm^{-1} that can be assigned to CH deformation modes that are unspecific and ring vibrations similar to those of 1,8-cineole. It is supposed that these differences between the measured and the calculated spectra are because not all compounds are taken into account. The resulting weighting factors for the three essential oils are 69.1% for 1,8-cineole, 12.2% for α-pinene, and 12.17% for limonene. The numbers obtained show a reasonable agreement with concentration data obtained by the GC methods (66.0 1,8-cineole, 17.3 α-pinene, 6.4 limonene). However, with more detailed information about the Raman scattering cross sections, a quantitative composition analysis by means of Raman spectroscopy should be possible. Furthermore, only three essential oils have been used for the analysis. We believe that if one would use a larger database of essential oils, the results could be improved further.

This discussion proves that main components of the analyzed *Eucalyptus* oils can be successfully investi-

Table II   Assignment for the Most Intensive Bands of Main Components in *Eucalyptus* Oils Identified by FT-Raman and ATR-IR Spectroscopy

Eucalyptus Species	FT-Raman (cm^{-1})	Component, Assignment	ATR-IR (cm^{-1})	Component, Assignment
E. jensenii	1625	Jensenone, ν (ring)	1625	Jensenone, ν (ring)
	1448	δ (CH$_3$), δ (CH$_2$)[a]	1593	Jensenone, ν (C=O)
			1421	Jensenone, δ (C—O—H)
			1190	Jensenone, ν (C—C—O)
E. macarthurii	1672	Geranyl acetate, ν (C=C)	1738	Geranyl acetate, ν (C=O)
	1441	δ (CH$_3$), δ (CH$_2$)[a]	1365	Geranyl acetate, δ_{sym} [CH$_3$(C=O)]
			1227	Geranyl acetate, ν_{as} (C—O—C)
			1021	Geranyl acetate, ν_s (C—O—C)
E. elata	1679	Terpinen-4-ol, ν (C=C)	1464	δ (CH$_3$), δ (CH$_2$)[a]
	1640	δ-2-*p*-Menthen-ol-1, ν (C=C)	1367	2-*p*-Menthen-ol-1, δ (C—O—H)
	1449	δ (CH$_3$), δ (CH$_2$)[a]	1123	2-*p*-Menthen-ol-1, ν (C—C—O)
	1208	*p*-Cymene, δ (*para*-disubstituted benzene)	924	Terpinen-4-ol, ω (CH$_2$)
	804	*p*-Cymene, δ (ring)		
	730	Terpinen-4-ol, δ (ring)		
E. torquata	1659	α-Pinene, ν (C=C)	1702	Torquatone, ν (ketone C=O)
	1448	δ (CH$_3$), δ (CH$_2$)[a]	1458	δ (CH$_3$), δ (CH$_2$)[a]
	666	α-Pinene, δ (ring)	1109	Torquatone, ν (C—O—C)
	652	1,8-Cineole, δ (ring)	984	1,8-Cineole, ω (CH$_2$)
E. citriodora	1725	Citronellal, ν (C=O)	1725	Citronellal, ν (C=O)
	1674	Citronellal, citronellol, ν (C=C)	1454	δ (CH$_3$), δ (CH$_2$)[a]
	1454	δ (CH$_3$), δ (CH$_2$)[a]	1377	Citronellol, δ (C—O—H)
	1382	Citronellal, citronellol, δ_{sym} (CH$_3$)	1116	Citronellal
E. crenulata	1701	γ-Terpinene, ν (nonconjugated C=C)	1736	Phenylethyl phenylacetate, ν (C=O)
	1613	*p*-Cymene, ν (ring)	1455	δ (CH$_3$), δ (CH$_2$)[a]
	1605	Phenylethyl phenylacetate, ν (ring)	1131	Phenylethyl phenylacetate, ν (C—O—C)
	1426	δ (CH$_3$), δ (CH$_2$)[a]	947	γ-Terpinene, ω (CH$_2$)
	1208	*p*-Cymene, δ (*para*-disubstituted benzene)	816	Phenylethyl phenylacetate, ω (C—H)
	1203	Phenylethyl phenylacetate, δ (ring)	698	Phenylethyl phenylacetate, δ (monosubstituted benzene)
	1003	Phenylethyl phenylacetate, δ (ring)		
	803	*p*-Cymene, δ (ring)		
	756	γ-Terpinene, δ (ring)		
E. polybractea	1447	δ (CH$_3$), δ (CH$_2$)[a]	1374	1,8-Cineole, δ_{sym} [CH$_3$(CO)]
	652	1,8-Cineole, δ (ring)	1214	1,8-Cineole, ν_{as} (C—O—C)
			1079	1,8-Cineole, ν_s (C—O—C)
			984	1,8-Cineole, ω (CH$_2$)
			843	1,8-Cineole
E. loxophleba	1678	Limonene, ν (cyclohexene C=C)	1374	1,8-Cineole, δ_{sym} [CH$_3$(CO)]
	1659	α-Pinene, ν (C=C)	1214	1,8-Cineole, ν_{as} (C—O—C)
	1447	δ (CH$_3$), δ (CH$_2$)[a]	1079	1,8-Cineole, ν_s (C—O—C)
	760	Limonene, δ (ring)	984	1,8-Cineole, ω (CH$_2$)
	667	α-Pinene, δ (ring)	843	1,8-Cineole
	652	1,8-Cineole, δ (ring)		
E. nortonii	1678	Limonene, α-terpineol, ν (cyclohexene C=C)	1374	1,8-Cineole, δ_{sym} [CH$_3$(CO)]
	1643	Limonene, ν (etylene C=C)	1214	1,8-Cineole, ν_{as} (C—O—C)
	1447	δ (CH$_3$), δ (CH$_2$)[a]	1079	1,8-Cineole, ν_s (C—O—C)
	760	Limonene, δ (ring)	984	1,8-Cineole, ω (CH$_2$)
	652	1,8-Cineole, δ (ring)	843	1,8-Cineole
E. globulus	1678	Limonene, ν (cyclohexene C=C)	[b]	[b]
	1659	α-Pinene, ν (C=C)		
	1447	δ (CH$_3$), δ (CH$_2$)[a]		
	760	Limonene, δ (ring)		
	667	α-Pinene, δ (ring)		
	652	1,8-Cineole, δ (ring)		
E. cinerea	652	1,8-Cineole, δ (ring)	[b]	[b]

[a] δ (CH$_3$), δ (CH$_2$) are characteristic for most components present in essential oils.
[b] Measurement was not performed.
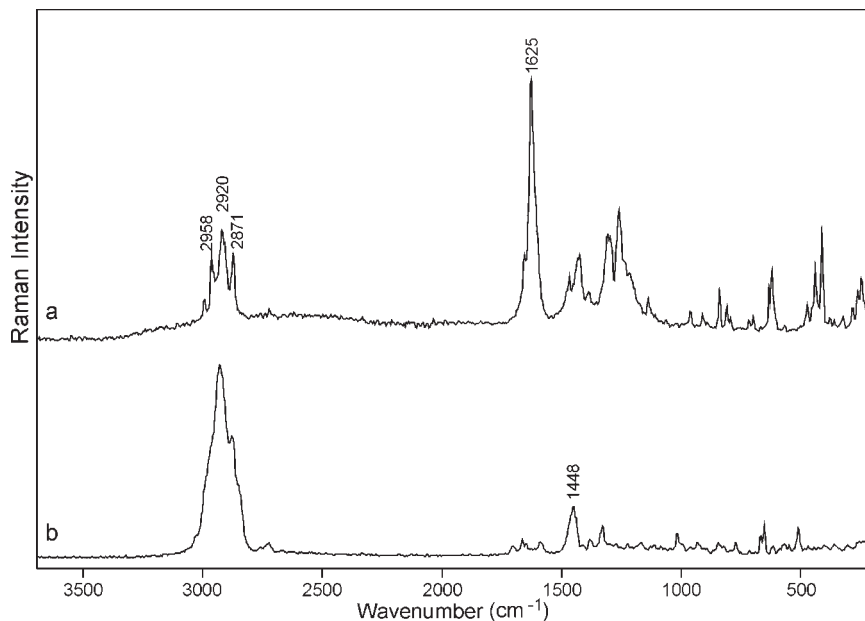
FIGURE 3 NIR-FT-Raman spectra of essential oils isolated by hydrodistillation from the leaves of *E. jensenii* (a) and *E. torquata* (b) in the wavenumber range between 3800 and 300 cm^{-1}.

gated by the complementary techniques of Raman and ATR-IR spectroscopy. Spectroscopic analysis based on the characteristic key bands of the individual volatile substances allow us to discriminate different essential oil profiles of the *Eucalyptus* species.

In Situ Investigation of *Eucalyptus* Essential Oil by Raman Mapping

A NIR-FT-Raman spectrometer with microequipment was used for the in situ analysis of essential oil in a
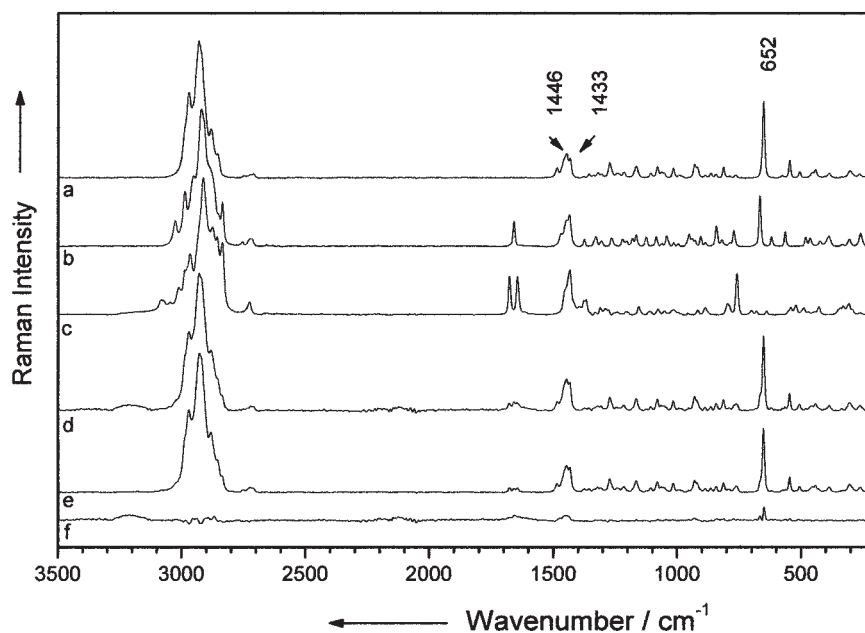
FIGURE 4 FT-Raman spectra of the standard substances 1,8 cineole (a), α-pinene (b), limonene (c), as well as an FT-Raman spectrum of *Eucalyptus loxophleba* (d), a weighted sum spectrum of 1.8 cineole, α-pinene, and limonene (e) and the difference spectrum (f) between the measured and the calculated spectrum of *E. loxophleba* (spectrum d − spectrum e).
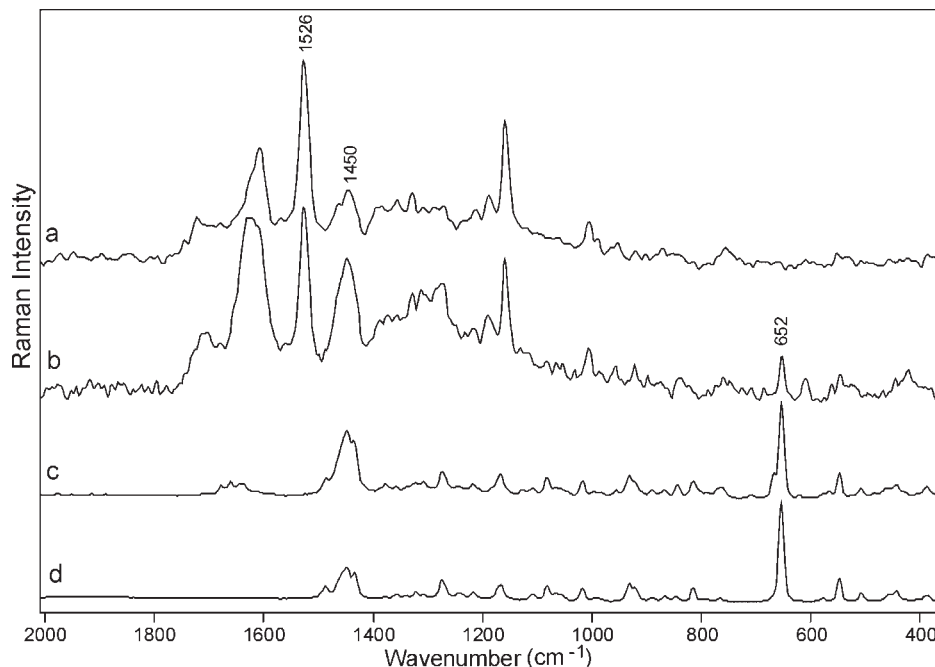
FIGURE 5   NIR-FT-Raman spectra taken from *Eucalyptus globulus* leaf, green area outside the oil droplet (a), oil droplet (b), essential oil isolated by hydrodistillation (c), and 1,8-cineole standard (d).

Eucalyptus globulus leaf. As can be seen in Figure 5, measurements were performed in the oil droplet (b), and for comparison, in the outside green area of the leaf as well (a). Furthermore, the spectrum of the essential oil isolated by hydrodistillation is also presented (c). GC analysis of this oil revealed that the main component is 1,8-cineole (about 50–60%); therefore the spectrum of this standard is demonstrated additionally (d). This bicyclocamphane compound shows a strong ring vibration at 652 cm^{-1} in the Raman spectrum that can be used for its identification. This marker band is clearly seen in the spectrum taken from the oil droplet (b) and proves that the in situ measurement was really performed in the essential oil cell. This is additionally confirmed by the increase of intensity of the band at 1450 cm^{-1}, which is the second intense band in the 1,8-cineole spectrum. Both spectra taken from the leaf show the presence of the plant matrix with the significant bands at 1525 and 1157 cm^{-1}, which are due to in-phase C=C (ν_1) and C—C (ν_2) stretching vibrations of the polyene chain of carotenoids.[20] In comparison to that, a spectrum taken in the oil droplet shows clearly lower intensity of the carotenoid signals.

More precise characterization of the *Eucalyptus* leaf can be performed by using a dispersive Raman spectrometer directly coupled with a microscope. Figure 6 presents an image of a leaf section of *Eucalyptus cinerea* taken through the microscope.

The Raman measurements were done in three characteristic spots marked in this picture. The small diameter of the laser used for this study (about 1 μm) allows precise investigation of the centre of the oil cavity (b), the green area of the leaf outside the droplet (a), as well as visible dark spots called "stomata" (c). A spectrum taken directly in the oil droplet shows the strong marker band of 1,8-cineole at 652 cm^{-1} and presents only weak carotene signals at 1526 and 1157 cm^{-1}. Contrary to that, a spectrum obtained from the green part of the leaf demonstrates mainly the presence of carotenoids. Quite different spectra are taken in the stomata (c), with significant bands allowing its identification as wax substances.[29] Signals at 1461 and 1439 cm^{-1} can be clearly attributed to CH$_3$ scissoring and asymmetrical bending modes, respectively. An intensive band at 1297 cm^{-1} is due to (CH$_2$)$_n$ in-phase twisting mode. Other Raman bands at 1127, 1062, and 888 cm^{-1} can be assigned as C—C stretching modes. Wax consists mainly of long aliphatic compounds and can be considered a mixture of esters, alkanes, and alkenes. In combination with cutin and suberin, wax forms protective cuticles that cover plant cell walls.[30] It provides a barrier for moisture diffusion in the plant and prevent the entry of microbial pathogens to the more easily degradable tissues within the leaves. The presence of wax in stomata has already been reported, e.g., for cere-
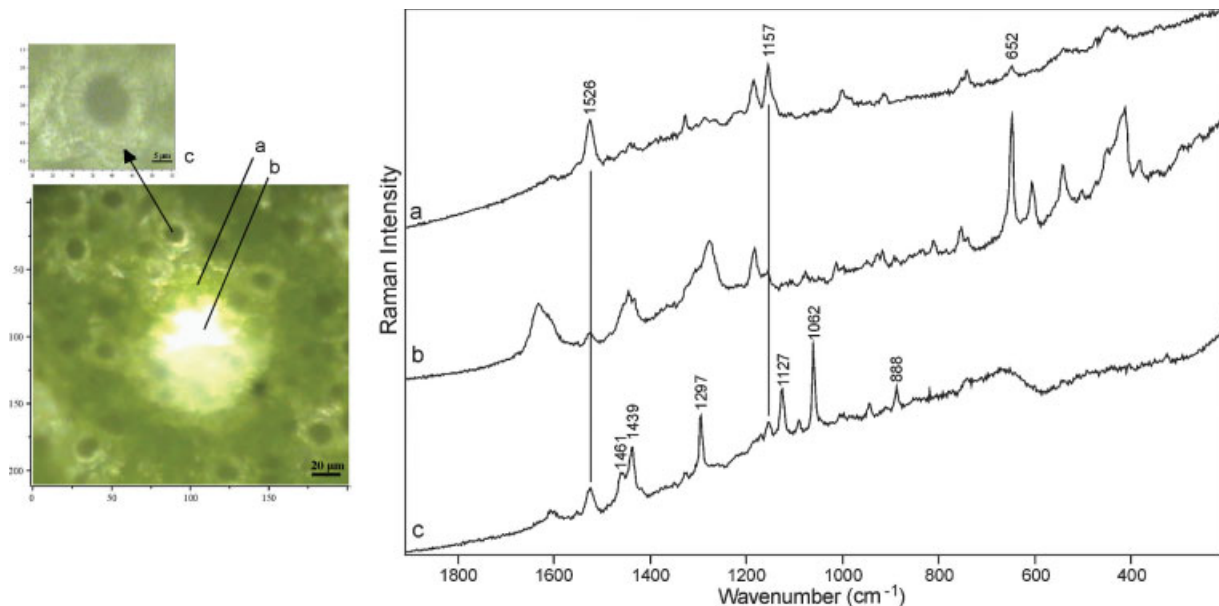
FIGURE 6   Images of a leaf section of *Eucalyptus cinerea* presenting the essential oil cavity and Raman spectra taken in the marked points, green area outside the oil cavity (a), oil cavity (b), and stomata (c).

als, where the occurrence of extensive wax covering of stomata was considered a resistance mechanism to fungi.[31]

The presence of characteristic 1,8-cineole bands in the spectrum of the oil droplet provide very good preconditions to apply Raman mapping for in situ investigation of the whole oil cavity visible in the eucalyptus leaf. In Figure 7A the microscopic image of a leaf section of *Eucalyptus cinerea* is presented. Integration of the band at 652 cm^{-1} provides information about the oil distribution, which is presented in Figure 7B (see Table I for details of oil composition). A big oil droplet visible in the centre is surrounded by small satellites covering an

area with a diameter of about 150 μm. Complementary to that, the Raman image obtained from integration of the signal at 1525 cm^{-1} shows the distribution of carotenoids in the measured area. Maximum amounts of carotenoids are seen outside the oil cavities and very low amounts are found in the range of the essential oil cells. Similar results can be obtained applying the micro NIR-FT-Raman equipment. The special advantage of this system is the possibility of measuring much bigger sample areas, but in comparison to the above-mentioned dispersive Raman arrangement, the resolution is lower. Figure 8A and B demonstrate the oil distribution in the region of 1200 × 1300 μm of *Eucalyptus*
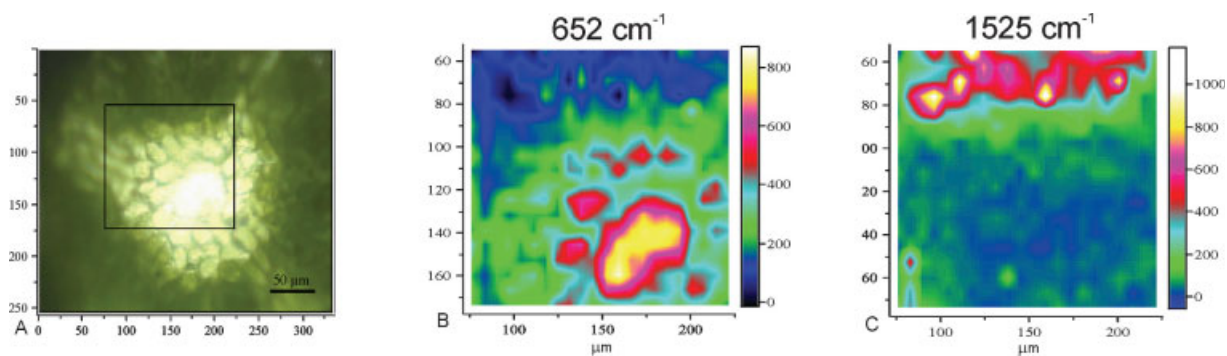
FIGURE 7   Microscopic image of a leaf section of *Eucalyptus cinerea* presenting the essential oil cavity (A) and Raman maps obtained from the defined area colored according to the intensity of the band at 652 cm^{-1} (B) and 1525 cm^{-1} (C) showing the distribution of essential oil (B) and carotenes (C).
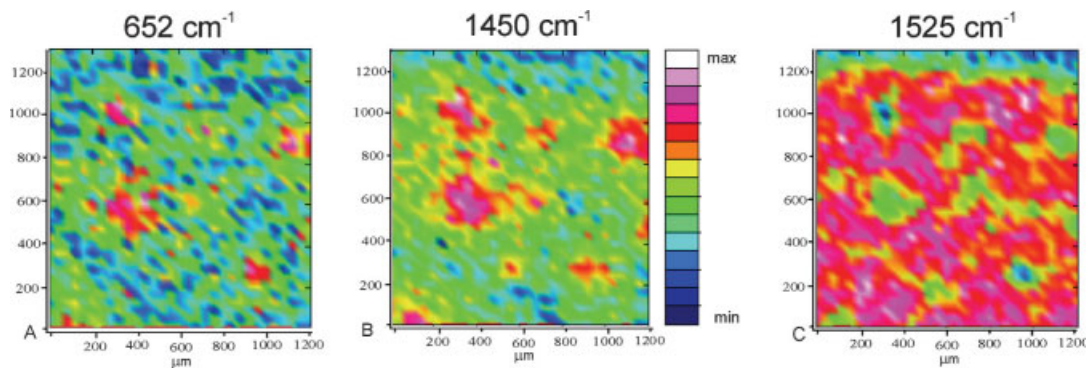
FIGURE 8 NIR-FT-Raman maps obtained from a *Eucalyptus globulus* leaf colored according to the intensity of the band at 652 cm^{-1} (A), 1450 cm^{-1} (B), and 1525 cm^{-1} (C) showing the distribution of essential oil (A and B) and carotenes (C).

globulus leaf colored according to the intensity of two most intensive bands of 1,8-cineole at 652 cm^{-1} (A) and 1450 cm^{-1} (B) (see Table I for details of oil composition). Again, the amount of carotenoids is lower in the spots where essential oil is present (Figure 8C), which corresponds to the results discussed above.

The obtained results demonstrate the usefulness of Raman mapping for in situ investigation of *Eucalyptus* oil distribution. Measurements within the oil cavity have revealed a decrease of carotenoid content in this part of the leaf. This observation, confirmed by both Raman techniques, has not been reported until now.

The investigation of the composition of *Eucalyptus* essential oil can be also performed with the mobile Raman setup. Figure 9 presents such a spectrum taken directly from the oil droplet from the leaf of *Eucalyptus globulus* (a) as well as the spectrum of the oil isolated by hydrodistillation (b). The marker bands of the main component of this oil, 1,8-cineole, are clearly seen in the in situ measurement whereas the bands from carotenoids are not present. Additional signals registered at 1632, 1275, 607, and 418 cm^{-1} are due to the plant matrix. The presented results show the potential of using the mobile Raman setup for field measurements, simplifying the whole analysis, in particular avoiding the transport of plants. On-site measurements can easily follow the changes of oil composition and help in determining the optimal harvesting time.
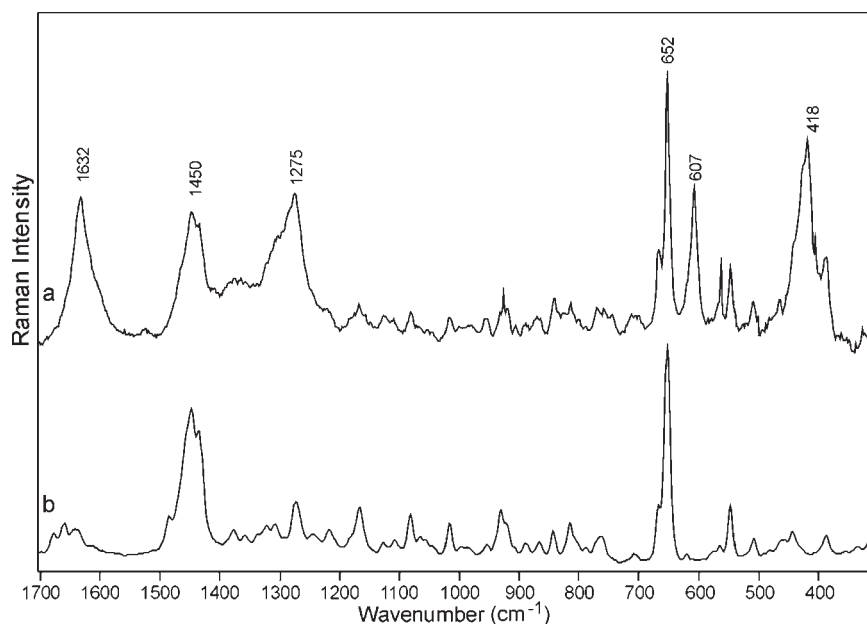
FIGURE 9 Raman spectrum of the essential oil of *Eucalyptus globulus* performed in situ with the mobile micro Raman setup (a). Additionally, spectrum of the isolated oil is also presented (b).

SUMMARY

The analysis of essential oils from several *Eucalyptus* species by using ATR-IR and NIR-FT-Raman spectroscopic methods is demonstrated. Both complementary spectroscopy techniques have the potential to replace existing standard procedures applied for quality control purposes. In particular, both methods can be used in the flavor and fragrance as well as in the pharmaceutical industry in order to perform fast quality checks of incoming raw materials and continuous controlling of distillation processes.

However, the isolation of essential oil can result in changes in its composition. Alternatively, in situ Raman measurements provide the possibility of nondestructive analysis of essential oil cells in the intact plant tissue without any sample preparation.

REFERENCES

1. Lassak, E. V.; McCarthy T. in Australian Medicinal Plants; North Ryde, NSW, Reed New Holland, 1983.
2. Lawler, I. R.; Eschler, B. M.; Schliebs, D. M.; Foley, W. J. J Chem Ecol 1999, 25, 2561–2573.
3. McLean, S.; Brandon, S.; Davies, N. W.; Foley, W. J.; Muller, H. K. J Chem Ecol 2004, 30, 19–36.
4. Ireland, B. F.; Goldsack, R. J.; Brophy, J. J.; Fookes, C. J. R.; Clarkson, J. R. J Essent Oil Res 2004, 16, 89–94.
5. Bignell, C. M.; Dunlop, P. J.; Brophy, J. J. Flav Frag J 1998, 13, 131–139.
6. Dunlop, P. J.; Bignell, C. M.; Jackson, J. F.; Hibbert, D. B. Chemom Intell Lab Sys 1995, 30, 59–67.
7. Heges, L. M.; Wilkins, C. L. J Chromatog Sci, 1991, 29, 345–350.
8. Krock, K. A.; Ragunathan, N.; Wilkins, C. L. Analyt Chem 1994, 66, 425–430.
9. Zini, C. A.; Augusto, F.; Christensen, E.; Smith, B. P.; Caramao, E. B.; Pawliszyn, J. Analyt Chem 2001, 73, 4729–4735.
10. Schulz, H.; Quilitzsch, R.; Krüger, H. J Mol Struct 2003, 661, 299–306.
11. Schulz, H.; Baranska, M.; Belz, H.-H.; Rösch, P.; Strehle, M. A.; Popp, J Vib Spectr 2004, 35, 81–86.
12. Schulz, H.; Schrader, B.; Quilitzsch, R.; Pfeffer, S.; Krüger, H. J Agric Food Chem 2003, 51, 2475–2481.
13. Schulz, H.; Schrader, B.; Quilitzsch, R.; Steuer, B. Appl Spectrosc 2002, 56, 117–124.
14. Schulz, H.; Drews, H.-H.; Krüger, H. J Essent Oil Res 1999, 11, 185–190.
15. Schulz, H.; Quilitzsch, R.; Drews, H.-H.; Krüger, H. Int Agrophysics 2000, 14, 249–253.
16. Martens, H.; Naes, T. Trac-Trends Anal Chem 1984, 3, 204–210.
17. Baranska, M.; Schulz, H.; Rösch, P.; Strehle, M. A.; Popp, J. Analyst 2004, 129, 926–930.
18. Strehle, M. A.; Rösch, P.; Baranska, M.; Schulz, H.; Popp, J. Biopolymers 2005, 77, 44–52.
19. Baranska, M.; Schulz, H.; Siuda, R.; Strehle, M. A.; Rösch, P.; Popp, J.; Joubert, E.; Manley, M. Biopolymers 2005, 77, 1–8.
20. Schulz, H.; Baranska, M.; Baranski, R. Biopolymers 2005, 77, 212–221.
21. European Pharmacopoeia, Maisonneuve SA, Sainte Ruffine, 1983.
22. Frisch, M. J.; Trucks, G. W.; Schlegel, H. B.; Scuseria, G. E.; Robb, M. A.; Cheeseman, J. R.; Zakrzewski, V. G.; Montgomery, J. A., Jr.; Stratmann, R. E.; Burant, J. C.; Dapprich, S.; Millam, J. M.; Daniels, A. D.; Kudin, K. N.; Strain, M. C.; Farkas, O.; Tomasi, J.; Barone, V.; Cossi, M.; Cammi, R.; Mennucci, B.; Pomelli, C.; Adamo, C.; Clifford, S.; Ochterski, J.; Petersson, G. A.; Ayala, P. Y.; Cui, Q.; Morokuma, K.; Rega, N.; Salvador, P.; Dannenberg, J. J.; Malick, D. K.; Rabuck, A. D.; Raghavachari, K.; Foresman, J. B.; Cioslowski, J.; Ortiz, J. V.; Baboul, A. G.; Stefanov, B. B.; Liu, G.; Liashenko, A.; Piskorz, P.; Komaromi, I.; Gomperts, R.; Martin, R. L.; Fox, D. J.; Keith, T.; Al-Laham, M. A.; Peng, C. Y.; Nanayakkara, A.; Challacombe, M.; Gill, P. M. W.; Johnson, B.; Chen, W.; Wong, M. W.; Andres, J. L.; Gonzalez, C.; Head-Gordon, M.; Replogle, E. S.; Pople, J. A. Gaussian 98, Revision A.11.4, Gaussian, Inc., Pittsburgh, PA, 2002.
23. Scott, A. P.; Radom, L. J Phys Chem, 1996, 100, 16, 502.
24. Boland, D. J.; Brophy, J. J.; Fookes, C. K. R. Phytochem 1992, 31, 2178–2179.
25. Baranska, M.; Schulz, H.; Krüger, H.; Qulitzsch, R. Anal Bioanal Chem 2005, 381, 1241–1247.
26. Daferera, D. J.; Tarantulis, P. A.; Polissiou, M. G. J Agric Food Chem 2002, 50, 5503–5507.
27. Lin-Vien, D.; Colthup, N. B.; Fateley, W. G.; Grasselli, J. G. in The Handbook of Infrared and Raman Characteristic Frequencies of Organic Molecules; Academic Press: San Diego, 1991.
28. Zborowski, K.; Ma'nuel, D. J.; Strommen, D. P.; Proniewicz, L. M. Vib Spectr 2001, 25, 7–17.
29. Strehle, M. A.; Jenke, F.; Fröhlich, B.; Tautz, J.; Riederer, M.; Kiefer, W.; Popp, J. Biopolymers 2003, 72, 217–224.
30. Stern, K. R.; Jansky, S.; Bidlack J. E. in Introductory Plant Biology; McGraw-Hill: New York, 2003; pp 60, 112.
31. Patto, M. C. V.; Rubiales, D.; Martin, A.; Hernandez, P.; Lindhout, P.; Niks, R. E.; Stam, P. Theor Appl Genet 2003, 106, 1283–1292.

Reviewing Editor: George J. Thomas